23rd ABCM International Congress of Mechanical Engineering
December 6-11, 2015, Rio de Janeiro, RJ, Brazil

EVALUATION OF THE LUBRICATION CONDITIONS IN THE INTERACTION BETWEEN PISTON AND CYLINDER

Lucas Tavares Selegatto[1]
Gregory Bregion Daniel[1]
[1]Laboratory of Rotating Machinery – Faculty of Mechanical Engineering – Postal Box 6122
University of Campinas (UNICAMP)
13083-970, Campinas, SP, Brazil
ltselegatto@fem.unicamp.br
gbdaniel@fem.unicamp.br

Abstract. *The pursuit for more efficient vehicles has been a research field over the last few years in order to obtain a reduction in both fuel consumption and the release of pollutants to the environment. In this context, hydrodynamic lubrication has played an important role, since it tends to reduce the friction, that is a main cause of wear and power loss in internal combustion engines. Therefore, this work aims to evaluate the lubrication conditions in automotive pistons, due to its importance and great influence in the performance of engines. For this, a mathematical model is developed taking into account two translational and two rotational motions to the piston within the cylinder. From these four degrees of freedom, the oil film thickness is determined and, consequently, the pressure distribution and the hydrodynamic forces acting on the piston can be evaluated. The results obtained in this work show the pressure distribution, the peak position of the maximum pressure and the hydrodynamic forces for different operational conditions. Due to the critical operational conditions, an estimation of the hydrodynamic forces is very important, since they act directly on the engine dynamic behavior. Finally, the model developed in this work can be successfully employed to estimate the hydrodynamic forces acting on the piston, being very important for the dynamic modeling of the slider-crank mechanism in internal combustion engines.*

Keywords: *Hydrodynamic Lubrication, Hydrodynamic Forces, Piston Skirt, Slider-Crank Mechanism*

1. INTRODUCTION

The internal combustion engines represent a highly complex mechanical system, since its correct operation involves many parameters, such as thermal efficiency of combustion, dynamic behavior of the assembly and lubrication of the components. The lubrication conditions in internal combustion engines have been research topic in recent years due to be related to frictional losses and wear of the components, i.e. affecting directly the efficiency and durability of the internal combustion engines.

The main energy losses in internal combustion engines occur in the set of power generation, composed by valves, cylinder, piston and journal bearings (Heywood, 1988; Jóvai and Maslov, 1973). Among these components stands out the piston which can represent up to 55% of energy loss (Richardson, 2000).

According to Cho and Moon (2005), the piston has a great influence on the internal combustion engine, affecting the most important performance indicators, such as efficiency, noise and energy consumption. For this reason, many researchers have studied the lubrication conditions between piston and cylinder, especially on the piston ring (Dowson et al., 1979; Priest et al., 1996; Han and Lee, 1998) and on the piston skirt (Knoll and Peeken, 1982; Dong et al. 1992; He et al., 2014).

In relation to the piston skirt, important studies have been developed in recent years. Yang et al. (2001) showed that the clearance and piston skirt length are very important parameters to reduce frictional loss. Nobutaka et al. (2004) showed that an optimized profile of the piston skirt can reduce the slap excitation. Three years later, Kim et al. (2007) showed that piston skirt geometry can reduce the wear of the piston. Recently, He et al. (2014) showed that the piston skirt parameters can influence on the dynamics behavior of the piston.

In this context, this work aims to evaluate the lubrication conditions on the piston skirt due to the interaction between piston and cylinder. For this, a mathematical model was developed from Reynolds' equation in order to determine the pressure distribution and the reaction forces due to hydrodynamic lubrication. The solution of the Reynolds' equation is obtained from the Finite Volume Method (FVM), because the ratio between the length and diameter of the piston is about 1 (assumption of finite bearing). The equation of the oil film thickness was developed considering four degrees of freedom, being two degrees of freedom related to translation (x and y) and two degrees of freedom related to rotation (α_x and α_y) of the piston inside the cylinder. Finally, the main results presented in this work are the pressure distribution, hydrodynamic forces and the oil film thickness.

2. METHODOLOGY

The methodology developed in this work is based in the Reynolds' equation that is the theoretical basis of the hydrodynamic lubrication (Reynolds, 1886). This equation can be obtained from the Navier-Stokes equations, considering some assumptions (Dowson, 1962). Thus, the classical Reynolds' equation can be adapted to the hydrodynamic lubrication on piston as presented in Eq. (1):

$$\frac{\partial}{\partial x}\left(\frac{h^3}{\mu}\frac{\partial P}{\partial x}\right)+\frac{\partial}{\partial z}\left(\frac{h^3}{\mu}\frac{\partial P}{\partial z}\right)=6W\frac{\partial h}{\partial z}+12\frac{\partial h}{\partial t} \tag{1}$$

where P is the pressure distribution on the piston, μ is the absolute viscosity of the lubricant oil, h is the oil film thickness between the piston and the cylinder, W is the linear velocity of the piston, t is the time and (x,z) is the coordinate system, being the first coordinate the piston's circumference and the second coordinate the piston's length.

As previously described, the equation of the oil film thickness was developed considering four degrees of freedom, being two degrees of freedom related to translation (x and y) and two degrees of freedom related to rotation (α_x and α_y) of the piston inside the cylinder. Considering this condition, the oil film thickness can be obtained from geometrical parameters and operation conditions as presented in Eq. (2):

$$h(\theta)= C_{Rvar}+(e_x+L_{var}\sin(\alpha_y))\sin(\theta+\phi)-(e_y+L_{var}\sin(\alpha_x))\cos(\theta+\phi) \tag{2}$$

where θ is the angular position on the piston, ϕ is the attitude angle, α_x and α_y are the angular positions of the piston; e_x and e_y are the displacements of the piston, C_{Rvar} is the radial clearance between the piston and the cylinder and L_{var} is the axial position on the piston, varying from –L/2 to L/2, being L the piston's length.

It is important to highlight that the radial clearance between the cylinder and piston is not constant in the axial direction, i.e. the piston is not cylindrical. This assumption is normally used in piston's design in order to improve the hydrodynamic lubrication due to axial motion of the piston. Fig. (1) shows a schematic representation of the piston.

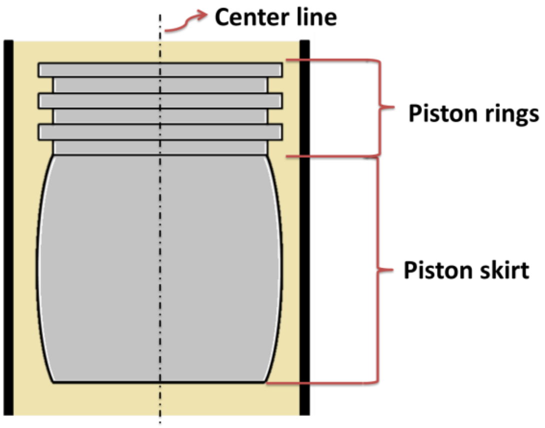

Figure 1: Schematic representation of the piston, showing the piston rings and the piston skirt.

A brief representation of the physical system is exposed in Fig. (2):

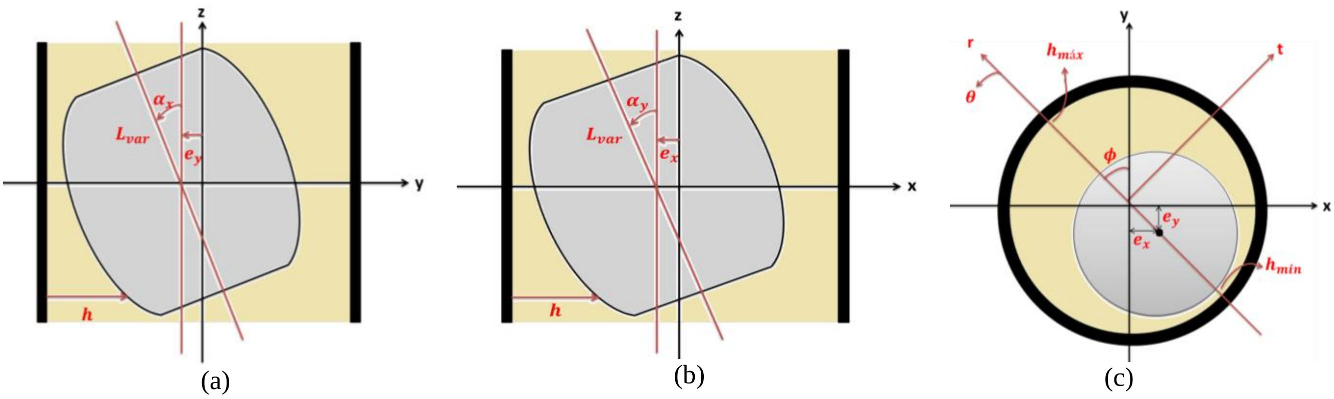

Figure 2: Scheme of the piston skirt and the cylinder. (a) View of the plan yz. (b) View.fo the plan xz. (c) View of the plan xy.

So, Eq. (1) can be solved to obtain the pressure distribution acting on the piston from the operational conditions and the geometric parameters. However, this equation (Reynolds' equation) is a non-homogeneous partial differential equation, whose analytical solution cannot be obtained for a finite bearing. Therefore, a numerical method must be applied in order to obtain the solution. In this paper, the Finite Volume Method (FVM) was applied as proposed by Maliska (2004).

In order to solve the equation through the Finite Volumes Method, a computational mesh was built to describe the external surface of the piston (problem domain). Figure 3 represents the computational mesh, emphasizing a control volume P, and the adjacent volumes, indicated by geographical coordinates (north: n; south: s; east: e; west: w).

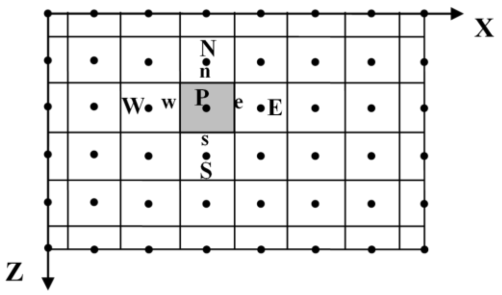

Figure 3: Computational mesh showing a control volume P in the surface of the piston.

The partial derivatives that describe the pressure gradient in the boundaries of the control volume can be approximated by the central differences scheme, as described in Eq. (3)

$$\frac{\partial}{\partial x}\left(\frac{h^3}{\mu}\frac{\partial P}{\partial x}\right) + \frac{\partial}{\partial z}\left(\frac{h^3}{\mu}\frac{\partial P}{\partial z}\right) = 6W\frac{\partial h}{\partial z} + 12\frac{\partial h}{\partial t} \tag{1}$$

$$\left.\frac{\partial P}{\partial X}\right|_e = \frac{P_E - P_P}{\Delta X} \quad ; \quad \left.\frac{\partial P}{\partial X}\right|_w = \frac{P_P - P_w}{\Delta X} \quad ; \quad \left.\frac{\partial P}{\partial Z}\right|_n = \frac{P_N - P_P}{\Delta Z} \quad ; \quad \left.\frac{\partial P}{\partial Z}\right|_n = \frac{P_P - P_S}{\Delta Z} \tag{3}$$

This way, the integration of the Reynolds' equation leads the linear equation presented below:

$$C_P P_P = C_E P_E + C_W P_W + C_N P_N + C_S P_S + B \tag{4}$$

In Eq. (4), the coefficients of each pressure (C_P, C_E, C_W, C_N and C_S) and the source term (B) are evaluated as:

$$\begin{aligned} &C_E = \frac{1}{\mu}\frac{\Delta z}{\Delta x} {h_e}^3; \quad C_W = \frac{1}{\mu}\frac{\Delta z}{\Delta x} {h_w}^3; \quad C_N = \frac{1}{\mu}\frac{\Delta x}{\Delta z}({h_n}^3); \quad C_S = \frac{1}{\mu}\frac{\Delta x}{\Delta z}({\bar{h}_s}^3); \\ &C_P = \frac{1}{\mu}\frac{\Delta z}{\Delta x}\left({h_e}^3 + {h_w}^3\right) + \frac{1}{\mu}\frac{\Delta x}{\Delta z}({h_n}^3 + {h_s}^3); \quad B = -6W[h_n - h_s] - 12\frac{\partial h}{\partial t}\Delta x \Delta z \end{aligned} \tag{5}$$

It is possible to verify that the source term is composed by two effects, wedge and squeeze. Thereby, squeeze effect in the source term is obtained from the variation of the film thickness over time. This way, the derivate of the film thickness can be obtained as proposed in Eq. (6):

$$\frac{\partial h}{\partial t} = \frac{\partial h}{\partial e_x}\frac{\partial e_x}{\partial t} + \frac{\partial h}{\partial e_y}\frac{\partial e_y}{\partial t} + \frac{\partial h}{\partial \alpha_x}\frac{\partial \alpha_x}{\partial t} + \frac{\partial h}{\partial \alpha_y}\frac{\partial \alpha_y}{\partial t} \tag{6}$$

The terms from Eq. (6) are evaluated by making use of Eq. (2). Then, the derivative can be written as:

$$\frac{\partial h}{\partial t} = \sin(\theta + \phi)\dot{e}_x - \cos(\theta + \phi)\dot{e}_y - L_{VAR}\cos(\alpha_x)\cos(\theta + \phi)\,\dot{\alpha}_x + L_{VAR}\cos(\alpha_y)\sin(\theta + \phi)\,\dot{\alpha}_y \tag{7}$$

Once the pressure distribution is already determined, the forces acting on the external surface of the cylinder can be obtained. Firstly, the hydrodynamic force acting in each volume of the mesh can be calculated. Afterwards, these forces can be summed according to the radial (r) and tangential (t) directions, as proposed in Eq. (8):

$$F_t = \sum_{i=1}^{N_x}\sum_{j=1}^{N_Z} P_P \sin(\theta)\,\Delta x \Delta z\ ; \quad F_r = \sum_{i=1}^{N_x}\sum_{j=1}^{N_Z} -P_P \cos(\theta)\,\Delta x \Delta z \tag{8}$$

Finally, the hydrodynamic forces in the x and y coordinates of the inertial system can be determined from the attitude angle as presented in Eq. (9):

$$F_x = F_t \cos(\phi) - F_r \sin(\phi); \quad F_y = F_t \sin(\phi) + F_r \cos(\phi) \tag{9}$$

When the piston has angular displacements related to the x and y axes (α_x and α_y), the center line of the piston is not parallel in relation to the z axis. Thus, the decomposition of force expressed in Eq. (9) should also include a component F_z. However, due to the values of the piston's length and the radial clearance, these angles (α_x and α_y) are very small, allowing this component to be neglected without considerable losses to the quality of the analysis. Moreover, the force generated by shear of the fluid film was not considered since the focus of this work is evaluate the reaction forces due to hydrodynamic lubrication that tends to avoid the contact between the piston and cylinder.

3. RESULTS

In order to analyze the model's behavior under real operation conditions, the numerical solution was implemented and some tests were performed.

During these tests, two groups of parameters were considered. The first group is named as physical parameters and it contains the geometrical dimensions used in the description of the system and also the absolute viscosity of the oil. This group was kept unchanged in all the tests. The second group is named as operational parameters, containing the conditions that can vary during the system's operation, such as the displacements and the velocities of the piston inside the cylinder. In order to simulate different condition, these parameters were altered through the tests, with exception of the linear velocity along *z*, kept in *-10m/s* in the whole set of tests.

The tables in the sequence show the physical and operational parameters of the model.

Table 1: Physical parameters adopted in the model to perform the tests.

Physical parameters	
$\mathbf{D_{CYLINDER}}$	70 mm
L	70 mm
$\mathbf{C_{r\_MAX}}$	60 µm
$\mathbf{\Delta C_r}$	30 µm
µ	0.05 Pa.s

Table 2: Operational parameters adopted in the model to perform the tests.

	Operational parameters								
Tests	W (m/s)	e_x (m)	e_y (m)	$\dot{e}_x$ (m/s)	$\dot{e}_y$ (m/s)	α_x (rad)	α_y (rad)	$\dot{\alpha}_x$ (rad/s)	$\dot{\alpha}_y$ (rad/s)
1	-10.00	0	0	0	0	0	0	0	0
2	-10.00	5.00E-06	0	0	0	0	0	0	0
3	-10.00	2.00E-05	0	0	0	0	0	0	0
4	-10.00	0	-1.00E-05	0	0	7.00E-04	0	0	0
5	-10.00	1.00E-05	1.00E-05	0	0	7.00E-04	7.00E-04	0	0
6	-10.00	1.00E-05	1.00E-05	1.00E-03	1.00E-03	7.00E-04	7.00E-04	7.00E-02	7.00E-02

The tests performed in this work generated different oil film thicknesses and, consequently, pressure distributions. These pressure distributions were obtained from the solution of the Reynolds' equation, in which the Finite Volumes Method was applied considering a computational mesh composed by 6400 volumes (80 volumes per direction). Moreover, the numerical solution was obtained considering the Gümbel's cavitation condition. The results obtained for each test is presented in following.

Figure 4(a) shows the pressure distribution in a condition where the eccentricity and its velocity are null (i.e. the piston is concentric with the cylinder), but the piston moves in a linear speed of *-10m/s* along *z* direction. This condition generated a pressure distribution that is constant in the circumferential direction, for each position on *z* direction (piston's length). This is expected since the oil film thickness is the same around the piston, indicating that there was hydrodynamic pressure due to oil wedge in z direction even without displacements in the directions *y* and *x*. It can be explained taking into account the piston skirt shape, whose radius varies along z direction, causing a positive wedge on first half and a negative wedge on second half for a positive velocity in z direction. For a negative velocity, the opposite behavior is observed. This shape generates a compression of the lubricant oil by forcing it through an area that decreases until the mid-line of the piston skirt. It is important to highlight that this phenomenon happens with or without displacements of the piston along *y* or *x* directions, changing just its intensity. So, in a situation where they occur simultaneously, the resulting pressure should be a combination of their effects.

In Fig. 4(b), the oil film thickness around the piston is a result of its shape (barrel shape). At its extremities, the space filled by the lubricant is simply the maximum radial clearance while in the middle occurs the minimum value of the radial clearance, evaluated just by subtracting ΔC_r from C_{r_MAX}.

The other figures whose sub-indexes are (b) are obtained by the combination of the piston shape and the displacements applied (linear and angular), resulting in different film thicknesses. It is possible to observe a common format of these figures, where the middle has a smaller gap and the extremities a higher one, showing an important influence of the piston skirt shape, which can superimpose the effects of the angular and linear displacements.

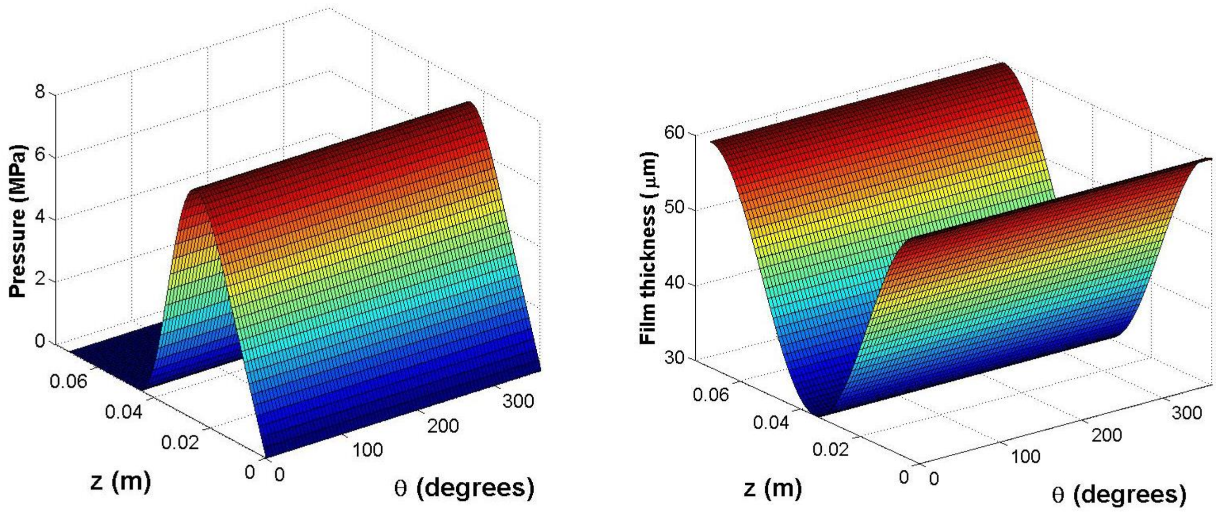

(a) (b)

Figure 4: Results obtained in test 1. (a) Pressure field. (b) Oil film thickness.

Figures 5(a) and 6(a) show the same condition, in which a linear speed of *10m/s* in *z* direction and a displacement causing an eccentricity in *x* direction are considered. The difference is only in the magnitude of such eccentricity. In the first case (Figure 5(a)), a small value (5 micrometers) is assumed while in the second case (Figure 6(a)) this value becomes four times greater (20 micrometers). Both situations show a clear increasing in the intensity of the oil wedge effect, caused by the approximation of the piston's external surface in relation to the cylinder's internal wall. Besides, Fig. 6(a) shows that when a radial displacement has the same order of magnitude of the radial clearance, the pressure peak tends to significantly overcome the pressure generated simply by the piston skirt shape.

The test that resulted in Fig. 7(a) is composed by two displacements in the plane *yz*: a negative linear (e_y) and a positive angular (α_x). Although Fig 2(a) was not made to represent this test, it can be used to visualize its configuration. From Fig 2(a), it is possible to verify that both displacements tend to decrease the gap between the piston and the cylinder above the *y* axis (superior region of the piston). Consequently, the fluid is more severely compressed in this region and the resulting pressure is greater. On the other hand, the effect observed is the opposite below the axis *y* (inferior region of the piston), increasing the gap between the surfaces, causing the oil compression and the pressure obtained (convergence region). This behavior depends on the displacements' signals.

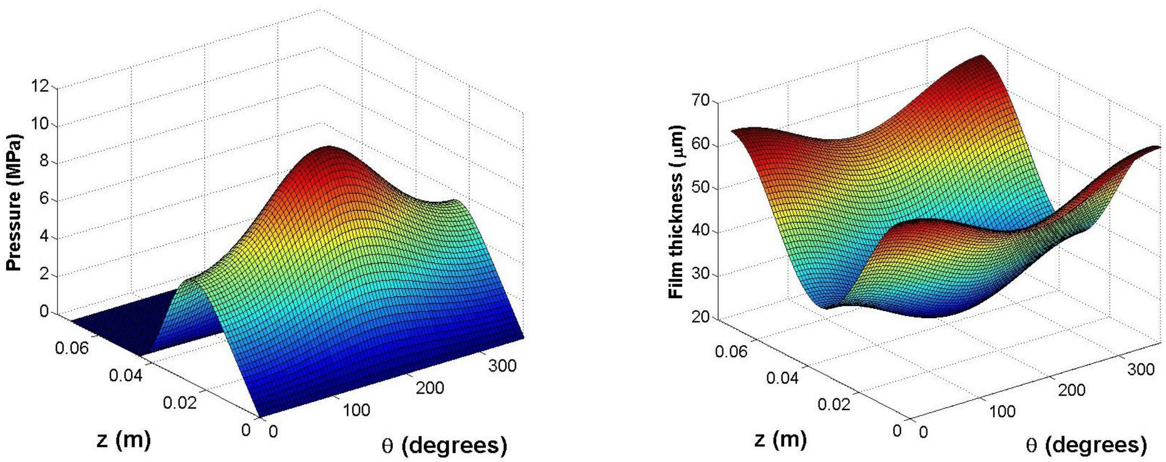

(a) (b)

Figure 5: Results obtained in test 2. (a) Pressure field. (b) Oil film thickness.

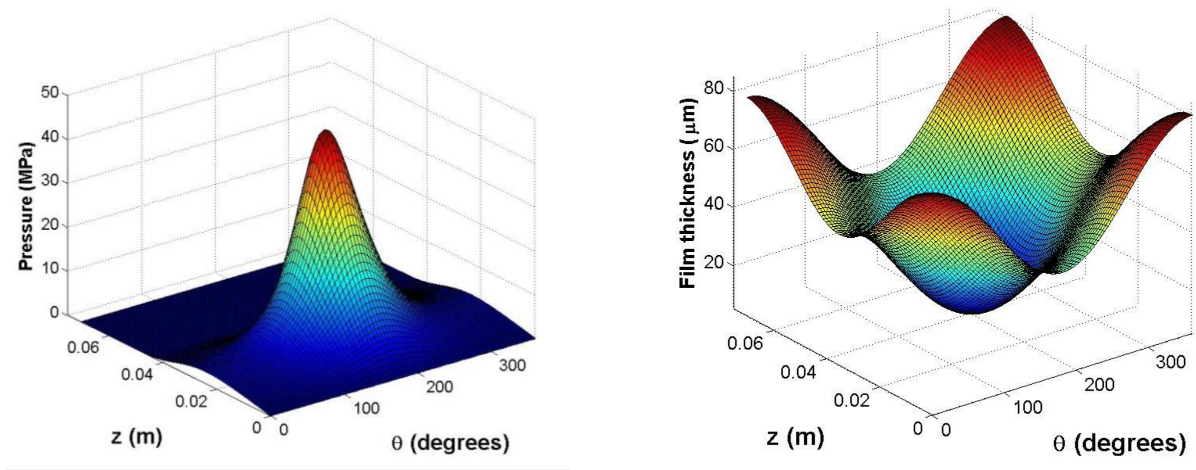

(a) (b)

Figure 6: Results obtained in test 3. (a) Pressure field. (b) Oil film thickness.

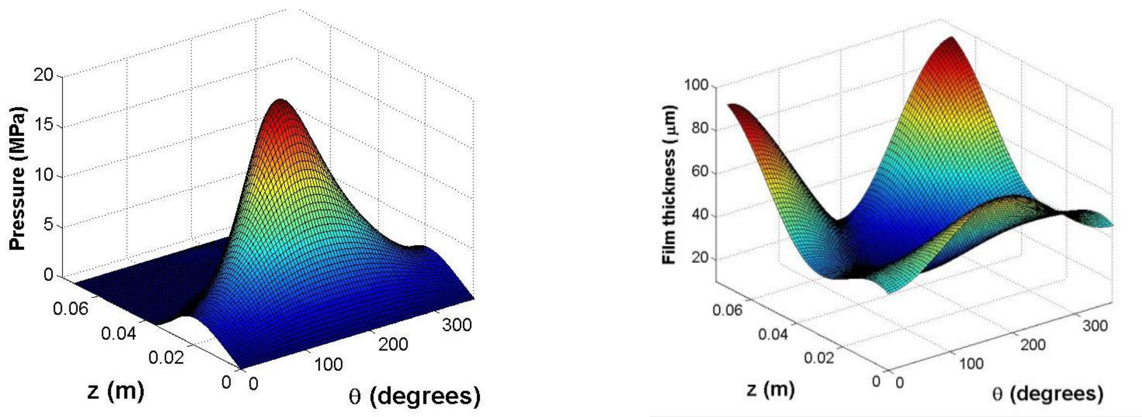

(a) (b)

Figure 7: Results obtained in test 4. (a) Pressure field. (b) Oil film thickness.

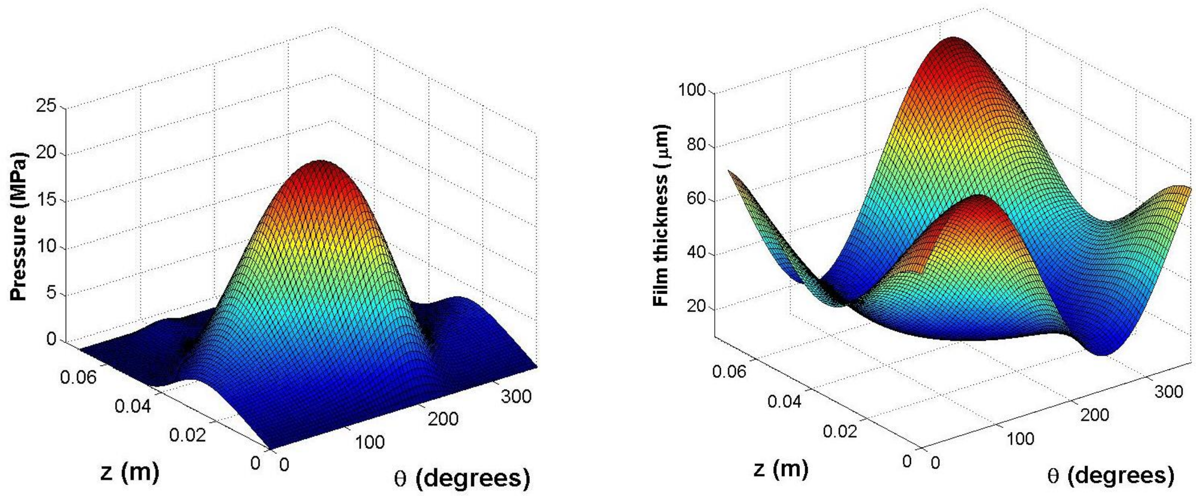

(a) (b)

Figure 8: Results obtained in test 5. (a) Pressure field. (b) Oil film thickness.

Lastly, Figs. 8(a) and 9(a) show the pressure distribution from the similar conditions. The eccentricities and the angular displacements are the same in both cases. Nevertheless, the first one has no velocity in the plane xy while in the second the piston has velocities in both directions of the plane xy and also angular velocities, as presented in table 2. Thus, the similarity of these figures allows to verify the influence of the velocities ($\dot{e}_x$, $\dot{e}_y$, $\dot{\alpha}_x$ and $\dot{\alpha}_y$) in the pressure distribution. In this work, there is a weak influence of these velocities in the pressure distribution. However, this behavior is consequence of the magnitude of the velocities considered in these simulations. Due to the dynamic of the system, the action of the combustion force and others effects, the piston's velocities in the plane *xy* can be higher, doing the squeeze effect more influent in the pressure distribution. In this scenario, the wedge and squeeze effects can have the same influence in the lubrication conditions in the interaction between piston and cylinder. Besides, a brief comment about the oil film thicknesses in the tests 6 and 7 (Figs. 8(b) and 9(b)) is necessary, since these results are exactly the same. It can be explained by the fact that the velocities in the plane *xy* can influence only the pressure distribution, due to the squeeze of the lubricant. On the other hand, the film thickness depends only on the position of the piston and the geometry of the system, characterized by the piston's skirt shape, piston's length, piston's diameter and cylinder's diameter.

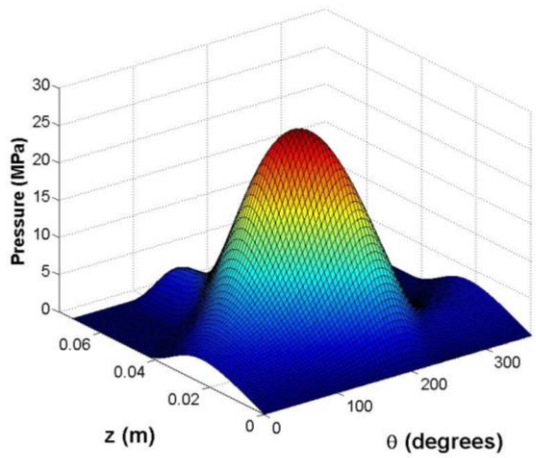

(a)

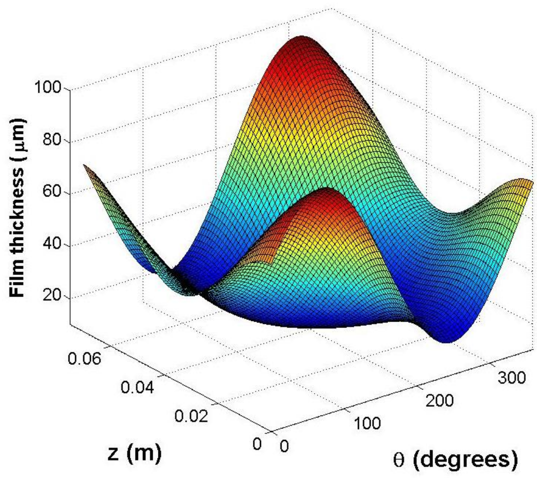

(b)

Figure 9: Results obtained in test 6. (a) Pressure field. (b) Oil film thickness.

In addition to the pressure distribution and oil film thickness, the hydrodynamic forces acting on the piston surface were also evaluated from the Eqs. (8) to (9). The following table shows these results for each one of the tests performed.

Table 3: Forces acting on the piston, for each test performed.

	Forces on the piston			
Tests	**F_r (N)**	**F_t (N)**	**F_x (N)**	**F_y (N)**
1	-1.33E-03	3.48E-05	-1.33E-03	3.48E-05
2	8.47E-03	5.80E+03	-5.80E+03	8.47E-03
3	3.30E-02	3.84E+04	-3.84E+04	3.30E-02
4	-1.61E-02	2.05E+04	-1.61E-02	2.05E+04
5	1.29E+04	2.05E+04	-2.36E+04	-5.38E+03
6	1.78E+04	2.87E+04	-3.29E+04	-7.66E+03

According to Table 3, the hydrodynamic forces acting in test 1 should be zero because the pressure distribution is constant along the circumferential direction. Analyzing the hydrodynamic forces obtained in tests 2 and 3, the hydrodynamic forces occur only in *x* direction, because the eccentricity was only considered in this direction. Moreover, the hydrodynamic force obtained in test 3 is greater due to the eccentricity considered in this test was four times greater than in test 2. Finally, the influence of the velocities in the plane *xy* can be verified from the hydrodynamic forces of the test 5 and 6.

4. CONCLUSION

This work aimed to study the lubrication in the interface between the piston skirt and the cylinder in internal combustion engines, more specifically the influence of the operational parameters. The Reynolds' equation was numerically solved to obtain the pressure distribution considering the wedge and squeeze effects in the oil film. Moreover, the fluid film thickness was also evaluated considering four degrees of freedom (translation: x and y; rotation: α_x and α_y).

From the numerical simulations, the results showed that for a given linear velocity along *z* direction, the piston skirt shape is responsible for generating a pressure distribution that is uniform in the circumferential direction of the piston and varies through its height. Thus, when the piston is centered in relation to the cylinder, this uniformity in the circumferential direction tends to cause hydrodynamic forces about null. On the other hand, in situations where the piston had non null values of eccentricities, the pressure distribution can be not uniform in the circumferential direction, since the oil film thickness is altered by the piston eccentricity, resulting hydrodynamic forces in the *xy* plane. The pressure distribution in these cases depends on the magnitude of the eccentricity. When the magnitude is similar to the piston radial clearance, the eccentricity effect tends to overcome the piston skirt shape effect. Configurations with smaller eccentricity lead to results similar the pressure distribution obtained with the piston centered. In addition, the hydrodynamic forces on the piston tend to increase when considered the velocities in plane *xy* (squeeze effect). However, the increasing depends on the magnitude of these velocities, being that for small magnitude the behavior practically does not change. Therefore, the simulation results offered a great understanding on how the operational parameters affect the pressure distribution and, consequently, the hydrodynamic forces over the piston.

Finally, the computation simulations performed in this work allow to conclude that this model can be extremely useful for analyzing the dynamic behavior of the slider-crank mechanism in the time domain, since the hydrodynamic forces acting on the piston should be evaluated and computed in the equation of motion of the system.

5. ACKNOWLEDGEMENTS

The authors would like to thank the CAPES for the financial support of this research.

6. REFERENCES

Cho, J.R., Moon, S.J., 2005. “A numerical analysis of the interaction between the piston oil film and the component deformation in a reciprocating compressor”. *Tribology International*, 38, pp. 459–468.

Dong Z., Cheng H S, Takayuki Arai, et al. ., 1992. “Numerical simulation analysis for piston skirts in mixed part lubrication – Part I: Basic modeling”. *ASME J Tribol*, 114:553–62.

Dowson, D., 1962. “A Generalized Reynolds Equation for Fluid Film Lubrication”, *International Journal of Mechanical Sciences*, Volume 4, Issues 2, pp. 159-170.

Dowson, D., Economou, P.N., Ruddy, B.L., Strachan, P.J., Baker, A.J.S., 1979. "Piston Ring Lubrication - Part II, Theoretical analysis of a single ring and a complete ring pack", *Energy Conservation Through Fluid Film Lubrication Technology: Frontiers in Research and Design*, ed. S.M. Rohde, D.F. Wilcock and H.S. Cheng, ASME pub., pp.23-52.

Han, D.-C., Lee, J.-S., 1998. “Analysis of the piston ring lubrication with a new boundary condition”, *Tribology International* Vol. 31, No. 12, pp. 753–760.

He, Z., Xie, W., Zhang, G., Hong, Z., Zhang, J., 2014. “Piston dynamic characteristics analyses based on FEM method Part I: Effected by piston skirt parameters”, *Advances in Engineering Software* 75, pp. 68–85.

Heywood, J. B., 1988. *Internal Combustion Engine Fundamentals*, McGraw-Hill.

Jóval, M. S., Máslov, G. S., 1973. *Motores de Automóvil*. Moscú: Editorial Mir.

Kim Kwang-soo, Godward Thom, Takiguchi Masaaki, et al., 2007. “The effects of lubricating oil film thickness distribution on gasoline engine piston friction”. SAE Paper 01-1247.

Knoll GD, Peeken HJ., 1982. “Hydrodynamic lubrication of piston skirts”. *ASME J Lub Technol*., 104:504–8.

Maliska, C. R., 2004, *Transferência de Calor e Mecânica dos Fluidos Computacional*, Livros Técnicos e Científicos Editora SA, Rio de Janeiro, RJ, Brasil, 2ª Ed.

Nobutaka T, Takayuki K, Keita H., 2004. “Optimization of profile for reduction of piston slap excitation”. SAE paper-01-4309.

Priest , M., Taylor, R.I., Dowson, D., Taylor C.M., 1996. “Boundary Conditions for Reynolds Equation with Particular Reference to Piston Ring Lubrication”, *The Third Body Concept, Elsevier Science* B.V., pp. 441-452.

Reynolds, O., 1886, “On the Theory of Lubrication and its Application to Mr. Beauchamp Tower's Experiments, including an Experimental Determination of the Viscosity of Olive Oil”. *Philosophical Transactions of Royal Society of London*, Series A, Vol. 177, Part 1, pp.157-234.

Richardson D., 2000. “Review of power cylinder friction for diesel engines”. *ASME J. Eng. Gas. Turb. in Power*, 122:506–19.

Yang JW, Yang W, Yu XD, et al., 2001” Design of internal combustion engine piston based on skirt lubrication analysis”. *SAE* paper 01-2486.

7. RESPONSIBILITY NOTICE